Influence of ENSO on stratospheric sulfur dioxide injection in the CESM2 ARISE-SAI-1.5 simulations

Chenrui Diao[1], Elizabeth A. Barnes[1], and James W. Hurrell[1]

[1]Department of Atmospheric Science, Colorado State University, Fort Collins, CO, USA

Corresponding to: Chenrui Diao (chenrui.diao@colostate.edu)

Key Points:

- The SAI controller applied in the CESM2 ARISE-SAI-1.5 simulation is significantly impacted by ENSO.

- The lagged response of the current SAI controller could lead to an increase in the variance of global mean surface temperature.

Abstract

16 Climate and Earth system models are important tools to assess the benefits and risks of
17 stratospheric aerosol injection (SAI) relative to those associated with anthropogenic climate
18 change. A "controller" algorithm has been used to specify injection amounts of sulfur dioxide in
19 SAI experiments performed with the Community Earth System Model (CESM). The experiments
20 are designed to maintain specific temperature targets, such as limiting global mean temperature
21 to 1.5ºC above the pre-industrial level. However, the influence of natural climate variability on
22 the injection amount has not been extensively documented. Our study reveals that more than
23 70% of the year-to-year variation in the total injection amount (excluding the long-term trend) in
24 CESM SAI experiments is attributed to the El Niño-Southern Oscillation (ENSO). A simplified
25 statistical model further suggests that the intrinsic, lagged response of the controller to the
26 climate can increase the variance of global mean temperature in the model simulations.

Plain Language Summary

28 As global temperatures rise due to increasing greenhouse gas (GHG) emissions, more attention
29 has been given to exploring the feasibility of stratospheric aerosol injection (SAI) as a means of
30 counteracting global warming. Several SAI simulations based on numerical climate models
31 utilize a "controller" algorithm to maintain global temperatures by adjusting aerosol injection
32 amounts on an annual basis. However, our findings reveal a strong influence of El Niño-
33 Southern Oscillation (ENSO) on the "controller" regarding the injection amounts. This
34 unexpected influence goes beyond the original design intent of the controller. Statistical analyses
35 further indicate that the current controller, while successfully preventing global warming, can
36 lead to an increased variance in global mean temperature.

1 Introduction

37 To mitigate global warming and projected future increases in weather and climate
38 extremes, greenhouse gas emissions must be dramatically reduced (Meinshausen et al., 2009;
39 IPCC, 2021). However, current and planned emission reductions will likely not be sufficient to
40 limit global warming to well under the 2ºC goal of the Paris Agreement. This motivates studies
41 exploring climate intervention (or 'geoengineering') as a possible approach to stabilize or reduce
42 global temperatures and possibly buy more time for emission reductions and the implementation
43 of climate adaptation measures. Stratospheric aerosol injection (SAI) may be one of the most
44 effective climate intervention approaches (e.g., Caldeira et al., 2013; NRC, 2015; Xu et al., 2020;
45 NASEM, 2021). By forming reflective aerosols in the stratosphere through injections of sulfate
46 particles (e.g., sulfur dioxide), SAI aims to reflect a small percentage of incoming solar radiation,
47 thus potentially offsetting greenhouse gas warming and minimizing some of the risks associated
48 with anthropogenic climate change.

49 Climate model simulations have been used to investigate both the benefits and potential
50 risks of SAI in the context of climate change (e.g., Kravitz et al., 2015; Mills et al., 2017; Richter
51 et al., 2022). MacMartin et al. (2014) introduced an SAI 'controller' algorithm to determine the
52 injection amounts and locations of sulfur dioxide needed each year to reach and maintain
53 prescribed temperature targets, such as the global mean surface temperature (GMST), the
54 hemispheric temperature gradient, and the pole-to-Equator temperature gradient (referred to as
55 T0, T1, and T2, respectively in Kravitz et al. 2017). To achieve this, at the end of each simulated
56 year, the controller calculates and compares the annual-mean values of GMST, T1, and T2 with

58 the respective values from the target climate period. A matrix calculation (based on the climate
59 sensitivity to SAI) is then applied to calculate the amount of sulfate particles needed at different
60 latitudes for the next year to offset the differences in GMST, T1, and T2 between the current
61 year and the target climate.

62 The National Center for Atmospheric Research (NCAR) recently released a new
63 ensemble of SAI experiments using the Community Earth System Model, version 2 (CESM2;
64 Danabasoglu et al. 2020), which also employed this controller algorithm (Richter et al. 2022).
65 The Assessing Responses and Impacts of Solar climate intervention on the Earth system with
66 Stratospheric Aerosol Injection (ARISE-SAI) results demonstrate the effectiveness of the
67 controller algorithm in maintaining the GMST at 1.5ºC above its pre-industrial value (Fig. S1a).
68 The ensemble-averaged sulfate injection amount in ARISE-SAI-1.5 shows a nearly-linear
69 increase with time, which resembles the increase in greenhouse gas (GHG) concentrations under
70 the moderate Shared Socioeconomic Pathway scenario of SSP2-4.5 scenario (O'Neill et al.,
71 2016) used in the simulations. However, the total injection amounts differ significantly across
72 individual ensemble members (Fig. S1b). This suggests that the controller may be responding not
73 only to the forced warming but also to inter-annual temperature fluctuations driven by model-
74 generated internal variability (thin blue lines in Fig. S1a). The El Niño-Southern Oscillation
75 (ESNO) is one of the most dominant modes of internal variability that influences both global as
76 well as regional climate (Ropelewski & Halpert, 1987; Wang et al., 2017). Thus, it is possible
77 that inter-annual variations in injection amounts are related to the controller's response to ENSO,
78 over and above the injection amounts needed to offset the externally-forced global warming.
79 Such responses might introduce unexpected fluctuations in both the SO_2 injection amount and
80 GMST.

81 Another issue related to the controller is the 'lagged response' intrinsic to the controller
82 algorithm. The injection amount determined by the controller for the following year is based on
83 the current year's climate. If ENSO influences the controller, the injection amount for the
84 following year will be calculated based on both the forced warming and the ENSO-driven
85 temperature changes from the current year. However, as the phase of ENSO can change quickly,
86 even by the following year (Stein et al., 2010). this may lead to a mismatch between the injection
87 amount and the ENSO-driven temperature variation. Consequently, the injection amounts may
88 not adequately maintain the temperature targets, or they may even exacerbate temperature
89 fluctuations in the following year. This mismatch may thus introduce potential side effects to
90 global and regional climate, particularly during years with quick transitions of ENSO.

91 Inspired by the two potential issues described above, we focus on two questions in this
92 study: (1) How much does ENSO impact the injection amounts determined by the controller; and
93 (2) to what extent does the lagged response of the controller affect the simulated climate?

2 Data and Methods

2.1 Model simulations

96 Our analyses are based on ensemble simulations using the Community Earth System
97 Model, version 2, with the Whole Atmosphere Community Climate Model, version 6
98 (CESM2(WACCM6); Danabasolgu et al., 2020). For studies of climate intervention using SAI,
99 representation of the entire stratosphere, including dynamics and chemistry, is needed to capture
100 the transport of stratospheric aerosols and their interactions with stratospheric constituents such

101 as water ozone and water vapor. Similarly, representing key processes and interactions between
102 multiple Earth system components is important, including coupling between the atmosphere,
103 land, ocean, and sea ice, as well as prognostic aerosols and interactive chemistry.

104 The ARISE-SAI experiments utilize a moderate emission scenario (SSP2-4.5) and
105 simulate SAI deployment in 2035 with a goal of keeping GMST near 1.5ºC above the pre-
106 industrial level (Richter et al. 2022). A 10-member ensemble of ARISE-SAI is compared to an
107 identical 10-member ensemble experiment without SAI (SSP2-4.5 hereafter). More technical
108 details can be found in Richter et al. 2022. We analyze monthly outputs of near-surface air
109 temperature (SAT) and sea surface temperature (SST).

110 The controller in ARISE-SAI injects sulfur dioxide (SO_2) into four one-grid boxes (15ºS,
111 15ºN, 40ºS, and 30ºN at 180º longitude) at an altitude of 21.6 km. In this study, we focus solely
112 on the total SO_2 injection amount, which is calculated by adding the amounts at all four injection
113 locations obtained from the controller log document. To investigate the year-to-year changes in
114 injection amount, we calculate the difference in the total SO_2 injection amount between the
115 following year and the current year (ΔSO_2 hereafter).

2.2 ENSO in the model simulations

117 As described earlier, year-to-year variations of the total SO_2 injection amount may be
118 related to model-generated internal variability, particularly that driven by ENSO. ENSO is a
119 dominant inter-annual mode of climate variability that strongly impacts global temperature (Cai
120 et al., 2015). Our focus, therefore, is on the potential impact of ENSO on the total injection
121 amount in ARISE-SAI.

122 We compute and examine the commonly-used Oceanic Niño Index (ONI; NOAA 2019)
123 to represent ENSO in CESM2 simulations. Specifically, a standardized ONI is calculated as the
124 3-month running mean of SST anomalies over the east-central tropical Pacific (5ºN–5ºS, 170ºW–
125 120ºW). The SST anomalies are relative to a 35-year base period from 2035 to 2069. Ensemble-
126 mean values of SST are subtracted from each simulation realization prior to the calculation in
127 order to remove the SST changes driven by external forcings. In order to be comparable with the
128 total sulfate injection amount, which varies annually, the annual mean of ONI is analyzed.

2.3 Simplified statistical model

130 The controller algorithm determines the SO_2 injection amount for the coming year based
131 on the annual mean temperatures of the past year. However, the GMST and the meridional
132 gradients in temperature for the coming year could differ significantly from the previous year
133 due to ENSO activity. To investigate how the lagged response of the controller influences the
134 variance of GMST in the simulations, we designed a simplified statistical model (SSM hereafter)
135 based on the GMST from the ARISE-SAI and the SSP2-4.5 simulations.

136 The SSM simplifies the climate system and considers GMST changes only. The GMST
137 in the SSM is set as follows: $T = T_{GHG} + T\_ENSO$, where T_{GHG} and T_{ENSO} represent the GHG
138 warming and the ENSO-driven GMST changes, respectively. To keep in line with the ARISE-

139   SAI and SSP2-4.5 experiments, the linear fit of the ensemble-mean GMST from the SSP2-4.5
140   experiment is applied to represent T_{GHG} (shown as dashed blue line in Fig. S2a).

141   In climate models and observations, ENSO-driven GMST changes occur over different
142   frequencies, and these may affect the climate impacts introduced by the controller's lagged
143   response. Therefore, to analyze the impacts of the lagged response on GMST variance given a
144   certain ENSO frequency, T_{ENSO} in the SSM is simplified to be an idealized monthly time series
145   with a specified variation frequency: $T_{ENSO} = A * sin(\omega t + \varphi)$, where A (the magnitude of
146   ENSO-driven GMST) is obtained based on the linear regression between ONI and detrended
147   GMST in the SSP2-4.5 simulation. The variation frequency and the initial condition of T_{ENSO} are
148   specified by changing the value of ω and φ, respectively. A sample T_{ENSO} with a 3-year
149   frequency is shown in Fig. S2a.

150   In response to SAI, the SSM has linear sensitivity to the sulfate injection amount, which
151   is calculated based on the linear regression between the total sulfate injection amount in ARISE-
152   SAI and the difference in GMST between SSP2-4.5 and ARISE-SAI (referred to as the "avoided
153   global warming"; Fig. S2b). We use the same controller algorithm in the SSM as is used in
154   ARISE-SAI. Since the SSM only considers GMST and has no spatial information, T1 and T2 are
155   fixed to the target values so that the controller does not respond to these two criteria. It is worth
156   noting that ENSO activity could also influence the sulfate injection locations by changing T1 and
157   T2. However, since our focus here is only on the total sulfate injection amount (which is
158   dominated by the GMST changes), it is reasonable to ignore these two indices in the SSM for
159   now.

160   **3 Results**

161   **3.1 Effects of ENSO on the SO$_2$ injection amount**

162   In addition to significant long-term warming induced by increases in GHG
163   concentrations, ENSO variations can also strongly influence GMST on interannual timescales.
164   This holds true in the ARISE-SAI simulations. Shown in Fig. 1 is the annual mean time series of
165   ONI, GMST anomalies above the pre-industrial level, as well as ΔSO_2 from all ten ensemble
166   members of ARISE-SAI. The average correlation between ONI and GMST is around 0.71,
167   which reveals that approximately 50% of the year-to-year variability of GMST in ARISE-SAI
168   can be attributed to variations of ENSO.

169   In addition, ΔSO_2 also shows significant year-to-year variation above the steadily
170   increasing injection amount that is required to counter increasing GHG forcing with time (orange
171   lines in Fig. 1). After the ramp-up period (first five years), when the controller initializes the
172   deployment with a mild increase in injection amounts to required values, the variability of ΔSO_2
173   is similar to that of GMST and ONI, and this is especially during strong ENSO events. Overall,
174   the correlation between ONI and ΔSO_2 is around 0.53. Since the controller determines the
175   injection amounts based on the annual mean GMST from the preceding year, it is clear that
176   ENSO strongly influences the controller's decision. In particular, compared to the total injection
177   amount (Fig. S1b), the year-to-year variation of ΔSO_2 accounts for about 5% to 10% of the total
178   injection amount in any given year, indicating that the controller's response to ENSO should be

179 large enough to detect even during the later period of ARISE-SAI (when the required injection
180 amount is far greater in order to counter the larger GHG forcing).

181   Although year-to-year variations of ΔSO_2 are highly correlated with ENSO, some large
182 values of ΔSO_2 are unrelated to ENSO-driven GMST changes (e.g., the first few years in
183 member 10; Fig. 1). Since only about 50% of the GMST variance is linearly associated with
184 ENSO, it is possible that other sources of internal variability may be affecting the variation of
185 ΔSO_2, a topic that is outside of the scope of this paper but is likely worthy of further exploration.

186   To further investigate inter-annual fluctuations of ΔSO_2, Fig. 2a shows the composite
187 map of surface air temperature (SAT) for times when the standardized ΔSO_2 time series is above
188 0.5 minus when it is below -0.5. The resulting composite pattern looks remarkably El Niño-like
189 (Cane & Zebiak, 1985). In particular, consistent with the high correlation between ENSO and
190 ΔSO_2 shown in Fig. 1, a strong El Niño (La Niña) event corresponds to a positive (negative)
191 ΔSO_2 , indicating the controller is changing its injection rates to offset the warm or cool anomaly
192 in GMST.

193   To quantify how much the composite map of ΔSO_2 can be explained by ENSO, a linear
194 regression between ΔSO_2 and ONI was constructed as: $\Delta SO_2 = \beta * ONI + r$, where $\beta * ONI$ is
195 the ENSO-driven ΔSO_2, and the residual (r) represents the non-ENSO driven changes in ΔSO_2.
196 About 72% (with a global pattern correlation between Fig. 2a and 2c of 0.85) of the SAT spatial
197 pattern driven by ΔSO_2 can be explained by the ENSO activity, which again emphasizes that
198 interannual variability of the total sulfate injection in ARISE-SAI are dominated by ENSO, an
199 aspect that yet to be documented.

200   After removing the linear effects of ENSO, the residual pattern of SAT (Fig. 2d) shows
201 warm anomalies over the middle-to-high latitudes of the Northern Hemisphere as well as over
202 tropical regions outside of the western tropical Pacific, reminiscent of a weak El Nino pattern.
203 This suggests that other modes of internal variability (e.g., the North Atlantic Oscillation or the
204 Pacific Decadal Oscillation) might also be important in affecting year-to-year variations of
205 ΔSO_2.

206 **3.2 Lagged response of the controller and increased GMST variance**

207   At the end of each simulated year, the ARISE-SAI controller calculates the injection
208 amounts needed for the next year based on the preceding year's annual mean temperature indices
209 (GMST, T1, and T2). However, since ENSO can change phases quickly within a single year, the
210 temperature indices, especially GMST (T0), might also change quickly in response to this ENSO
211 variability. In this situation, the previously determined injection amount may not adequately
212 satisfy the injection needs of the coming year, or, it may even exacerbate temperature
213 fluctuations.

214   The schematic diagram in Fig. 3a shows an idealized case of ENSO quickly transitioning
215 from a warm event in year one to a cold event in year two. By the end of the first year, the
216 controller would detect an ENSO-driven global warming anomaly and increase the injection
217 amount in the second year to offset not only the incremental GHG warming but also the warming
218 driven by El Niño. However, if a cold event (La Niña) occurs naturally in year two, the

219 controller's decision would lead to an even greater global cooling than would have otherwise
220 occurred without the controller. Similarly, in the case of ENSO quickly transitioning from a cold
221 event (La Niña) to a warm event (El Niño), the controller would decrease the injection amount
222 by too much and not adequately offset the GHG warming. It follows from this basic example that
223 the year-to-year variability of GMST might ultimately be larger than expected due to the
224 controller responding to ENSO variability. Fast ENSO transitions are apparent in both the
225 ARISE-SAI simulations (e.g., 2056–2057 in Member 004, and 2051–2052 in Member 005; Fig.
226 1) and in observations (e.g., 2010-2011; not shown).

227   To further examine how the controller's response to ENSO affects the variance of
228 GMST, we developed a simplified statistical model based on the ARISE-SAI and SSP2-4.5
229 simulations, in which the idealized "ENSO" signal has only one specific variation frequency (see
230 Section 2.3). When the variation frequency of ENSO is twice the controller's detection
231 frequency (i.e., two years, shown in Fig. 3b), the controller's decision follows the mechanism
232 described in Fig. 3a and leads to a 34% increase in the variance of GMST. However, this is an
233 extreme case, since ENSO typically varies from two to seven years.

234   We thus further explore the controller's decisions for different ENSO frequencies (Fig.
235 S3). The results show that the controller algorithm always introduces increased variance in
236 GMST, but the magnitudes of this additional variance depend strongly on the hypothetical ENSO
237 frequency. Specifically, when ENSO varies at relatively high frequencies (e.g., panels a and c in
238 Fig. S3), the GMST variance increases by more than 20%. At lower frequencies (such as seven
239 years in Fig. S3d), the controller can adequately account for most ENSO-induced GMST
240 changes, and it only introduces a small increase in the variance of GMST. In other words, the
241 lagged response of the controller is strongly impacted by the frequency of ENSO variability.

242   Considering the potential issue introduced by the lagged response of the controller, we
243 further test how the variance of GMST would change if the controller made injection decisions
244 on timescales other than annual. For instance, if the controller changed injection amounts every
245 two years (Fig. 4b), the variance of GMST would significantly increase, and GMST would still
246 slowly increase despite the continuous sulfate injection. More extreme cases occur when the
247 controller injects even less often, such as every five years (Fig. 4c). In this case, the controller
248 fails to offset the GHG warming because the injection amount is always behind the increasing
249 GHG concentrations.

250   A more intuitive way to prevent introducing spurious variance due to the controller's
251 lagged response would be to detect temperature indices more frequently than once-per-year.
252 Results from the SSM for a controller that changes injection amounts monthly are shown in Fig.
253 4d. In this case, the variance of GMST is decreased by about 30%, which means the controller
254 mutes part of the ENSO-driven GMST variation. However, muting ENSO-driven GMST
255 variability to such an extent might also introduce unexpected climate impacts both globally and
256 locally.

257   Comparing the GMST variance between the SSP2-4.5 and ARISE-SAI ensemble
258 simulations (Fig. 5a), it is clear that the averaged GMST variance in ARISE-SAI is greater than
259 that in SSP2-4.5 in both early and late periods (2040–2054 and 2055–2069), consistent with the
260 results from the SSM. Despite largely maintaining the mean values of temperature indices,

261 ARISE-SAI introduces significantly greater GMST variance compared to the climate of the
262 target period (2020–2034 in SSP2-4.5). The SSP2-4.5 simulations show a decrease in the GMST
263 variance because of GHG warming; however, variances across individual simulations exhibit a
264 large spread. Thus, due to the limited ensemble sizes (10 members in both the SSP2-4.5 and
265 ARISE-SAI cases), the variance comparison here contains large uncertainties. The results in Fig
266 5, therefore, are intriguing but are inconclusive on their own. Additional ensemble members
267 would be required to more confidently state that the lagged response of the controller is driving
268 the differences in GMST variance evident between the SSP2-4.5 and ARISE-SAI simulations.

269 **4 Conclusions and Discussion**

270 The controller algorithm in the ARISE-SAI simulations greatly accomplishes its primary
271 goal; that is, to offset GHG warming by maintaining GMST and meridional temperature
272 gradients at the target values. However, we have shown that the controller is also strongly
273 impacted by ENSO activity, and its lagged response to the temperature targets can introduce a
274 mismatch between injection amounts and ENSO-driven temperature variation, and thus, lead to
275 increases in GMST variance. This is especially true for the case when ENSO varies on similar
276 timescales to the controller's detection frequency (set at one year in the ARISE-SAI
277 simulations). Given these two factors, it may therefore be worthwhile to focus efforts on
278 distinguishing and removing GMST variations driven by ENSO from the algorithm, a topic of
279 ongoing work.

280 In addition, the residual map of the composite analysis in Fig. 2d suggests that other
281 modes of internal climate variability may also disturb the controller, although with smaller
282 magnitudes than that due to ENSO. Additional analyses involving the hemispheric temperature
283 gradient and the equator-to-pole gradient (T1 and T2) could be beneficial to further understand
284 the controller's behavior in response to such modes.

285 Lastly, we have focused on the global mean temperature in this study. Additional analysis
286 is warranted to determine whether the controller's response to ENSO introduces detectable
287 regional climate impacts.

288

295 **Open Research**

296 The CESM2-WACCM6-SSP2-4.5 (https://doi.org/10.26024/0cs0-ev98) and CESM2-

297 WACCM6-ARISE-SAI-1.5 (https://doi.org/10.5065/9kcn-9y79) simulations applied in this study

298 are produced and maintained by the National Center for Atmospheric Research (NCAR), both of

299 which are publicly available from: https://www.cesm.ucar.edu/community-projects/arise-sai. All

300 Python codes related to this study are available at https://github.com/C-R-

301 Diao/ARISE_Controller_ENSO. At the time of publication, the codes will be converted to a

302 permanent repository on Zenodo.

303

304 **References**

305 Ben Kravitz, Douglas G. MacMartin, Michael J. Mills, Jadwiga H. Richter, Simone Tilmes,

306   Jean-Francois Lamarque, Joseph J. Tribbia, Francis Vitt. (2017). First Simulations of

307   Designing Stratospheric Sulfate Aerosol Geoengineering to Meet Multiple Simultaneous

308   Climate Objectives. *Journal of Geophysical Research: Atmospheres*, *122*(23), 2169–

309   2897X.

310 Cai, W., Santoso, A., Wang, G., Yeh, S.-W., An, S.-I., Cobb, K. M., Collins, M., Guilyardi, E.,

311   Jin, F.-F., Kug, J.-S., Lengaigne, M., McPhaden, M. J., Takahashi, K., Timmermann, A.,

312   Vecchi, G., Watanabe, M., & Wu, L. (2015). ENSO and greenhouse warming. *Nature*

313   *Climate Change*, *5*(9), 849–859.

314 Cane, M. A., & Zebiak, S. E. (1985). A Theory for El Niño and the Southern Oscillation.

315   *Science*, *228*(4703), 1085–1087.

316 Kravitz, B., Robock, A., Tilmes, S., Boucher, O., English, J. M., Irvine, P. J., Jones, A.,

317   Lawrence, M. G., MacCracken, M., Muri, H., Moore, J. C., Niemeier, U., Phipps, S. J.,

318   Sillmann, J., Storelvmo, T., Wang, H., & Watanabe, S. (2015). The Geoengineering

319   Model Intercomparison Project Phase 6 (GeoMIP6): simulation design and preliminary

320   results. *Geoscientific Model Development*, *8*(10), 3379–3392.

321   MacMartin, D. G., Kravitz, B., Keith, D. W., & Jarvis, A. (2014). Dynamics of the coupled

322   human–climate system resulting from closed-loop control of solar geoengineering.

323   *Climate Dynamics*, *43*(1), 243–258.

324   Meinshausen, M., Meinshausen, N., Hare, W., Raper, S. C. B., Frieler, K., Knutti, R., Frame, D.

325   J., & Allen, M. R. (2009). Greenhouse-gas emission targets for limiting global warming

326   to 2 degrees C. *Nature*, *458*(7242), 1158–1162.

327   Mills, M. J., Richter, J. H., Tilmes, S., Kravitz, B., MacMartin, D. G., Glanville, A. A., Tribbia,

328   J. J., Lamarque, J.-F., Vitt, F., Schmidt, A., Gettelman, A., Hannay, C., Bacmeister, J. T.,

329   & Kinnison, D. E. (2017). Radiative and chemical response to interactive stratospheric

330   sulfate aerosols in fully coupled CESM1(WACCM). *Journal of Geophysical Research*,

331   *122*(23), 13,061–13,078.

332   National Academies of Sciences, Engineering, and Medicine. (2021). *Reflecting Sunlight:*

333   *Recommendations for Solar Geoengineering Research and Research Governance.*

334   National Academies Press.

335   National Oceanic and Atmospheric Administration. (2019). *Cold & Warm Episodes by Season*.

336   https://origin.cpc.ncep.noaa.gov/products/analysis_monitoring/ensostuff/ONI_v5.php

337   National Research Council. (2015). *Climate Intervention: Reflecting Sunlight to Cool Earth*.

338   National Academies Press.

339   O'Neill, B. C., Tebaldi, C., van Vuuren, D. P., Eyring, V., Friedlingstein, P., Hurtt, G., Knutti,

340   R., Kriegler, E., Lamarque, J.-F., Lowe, J., Meehl, G. A., Moss, R., Riahi, K., &

341   Sanderson, B. M. (2016). The Scenario Model Intercomparison Project (ScenarioMIP)

342   for CMIP6. *Geoscientific Model Development*, *9*(9), 3461–3482.

343   Richter, J. H., Visioni, D., MacMartin, D. G., Bailey, D. A., Rosenbloom, N., Dobbins, B., Lee,

344   W. R., Tye, M., & Lamarque, J.-F. (2022). Assessing Responses and Impacts of Solar

345   climate intervention on the Earth system with stratospheric aerosol injection (ARISE-

346   SAI): protocol and initial results from the first simulations. *Geoscientific Model*

347   *Development*, *15*(22), 8221–8243.

348   Ropelewski, C. F., & Halpert, M. S. (1987). Global and Regional Scale Precipitation Patterns

349   Associated with the El Niño/Southern Oscillation. *Monthly Weather Review*, *115*(8),

350   1606–1626.

351   Stein, K., Schneider, N., Timmermann, A., & Jin, F.-F. (2010). Seasonal Synchronization of

352   ENSO Events in a Linear Stochastic Model. *Journal of Climate*, *23*(21), 5629–5643.

353   Tilmes, S., Richter, J. H., Kravitz, B., MacMartin, D. G., Mills, M. J., Simpson, I. R., Glanville,

354   A. S., Fasullo, J. T., Phillips, A. S., Lamarque, J.-F., Tribbia, J., Edwards, J., Mickelson,

355   S., & Ghosh, S. (2018). CESM1(WACCM) Stratospheric Aerosol Geoengineering Large

356   Ensemble Project. *Bulletin of the American Meteorological Society*, *99*(11), 2361–2371.

357   Wang, C., Deser, C., Yu, J.-Y., DiNezio, P., & Clement, A. (2017). El Niño and Southern

358   Oscillation (ENSO): A Review. In P. W. Glynn, D. P. Manzello, & I. C. Enochs (Eds.),

359   *Coral Reefs of the Eastern Tropical Pacific: Persistence and Loss in a Dynamic*

360   *Environment* (pp. 85–106). Springer Netherlands.

361   Xu, Y., Lin, L., Tilmes, S., Dagon, K., Xia, L., Diao, C., Cheng, W., Wang, Z., Simpson, I., &

362   Burnell, L. (2020). Climate engineering to mitigate the projected 21st-century terrestrial

363   drying of the Americas: a direct comparison of carbon capture and sulfur injection. *Earth*

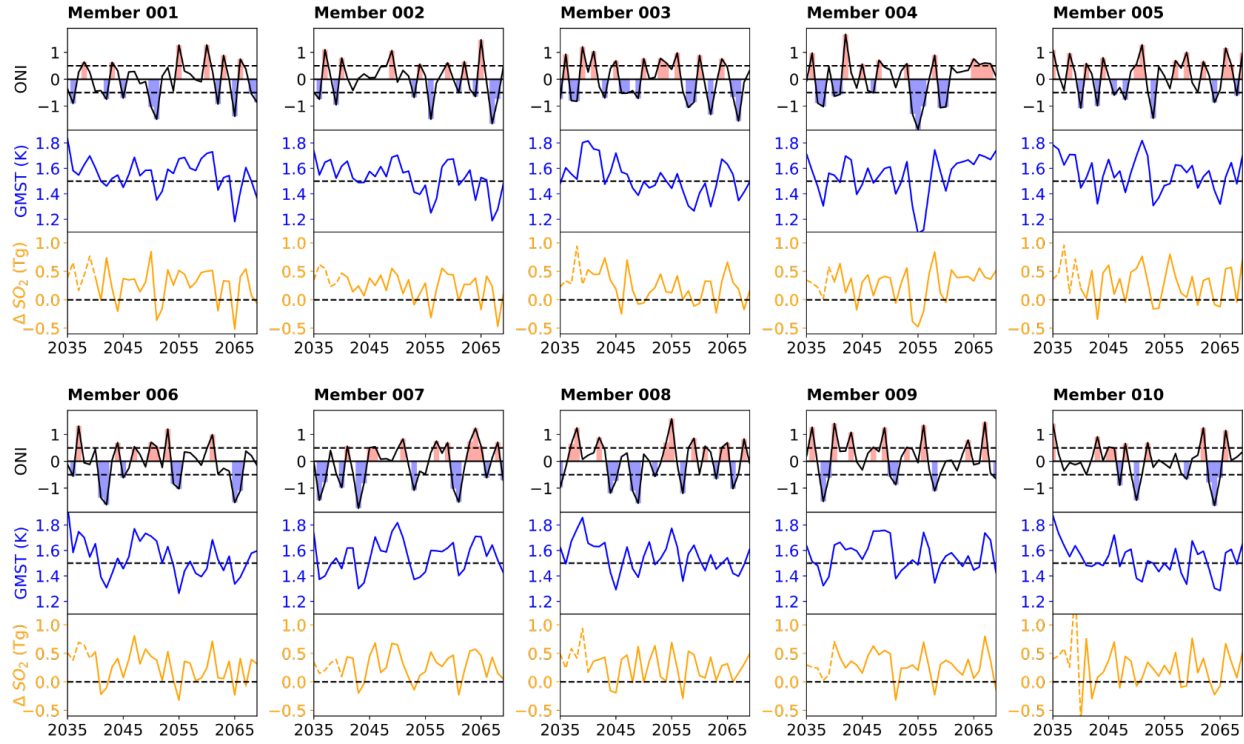364   *System Dynamics*, *11*(3), 673–695.

Figure 1. The annual-mean time series of (upper) Oceanic Niño Index (ONI), (middle) GMST anomalies above the pre-industrial level, and (lower) ΔSO_2 for each realization in ARISE-SAI simulation. The annual ONI anomalies are calculated based on the average of monthly ONI; years with ONI anomalies greater than 0.5 ºC (less than -0.5ºC) are marked with red (blue) bars. The first five years (1935–1939, shown as dashed lines in ΔSO_2 panels) are the ramp-up periods according to the controller algorithm.

Figure 2. (a) The composite map of surface air temperature (SAT) anomalies in ARISE-SAI when ΔSO_2 (standardized) is greater than 0.5 compared to when ΔSO_2 is less than -0.5. Composite samples are picked from all ensemble members. (b) Linear regression between standardized ONI and ΔSO_2 based on all ten realizations from ARISE-SAI. (c) Same as panel (a) but for ENSO-driven ΔSO_2 calculated from the linear regression in panel (b). (d) The residual map of (a) - (c)
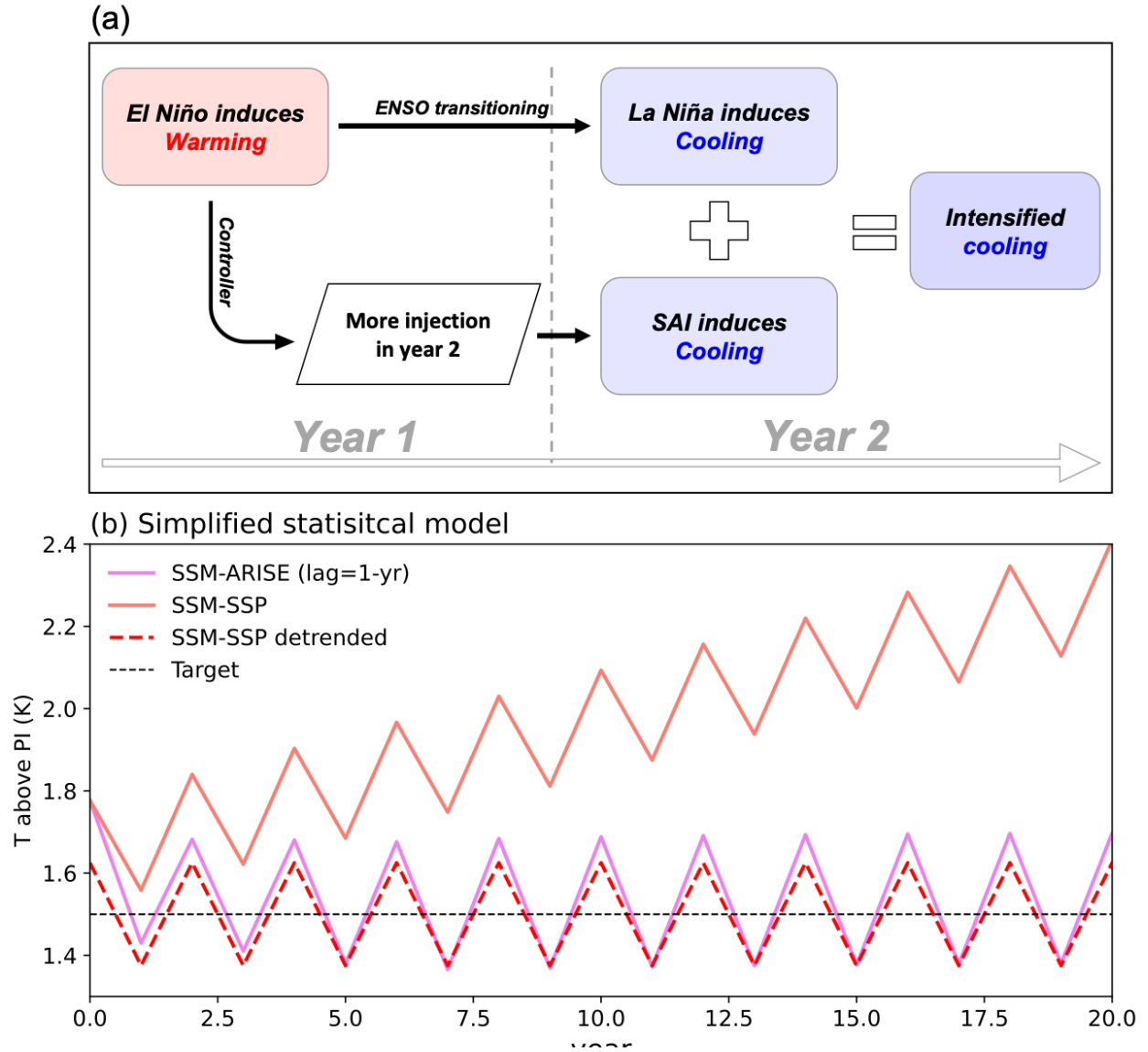
(a)

(b) Simplified statisitcal model

Figure 3. (a) Schematic of intensified cooling during an ENSO quick transitioning case. (b) The results of climate intervention in the simplified statistical model (SSM; see Section 2.3) with idealized "ENSO" at a fixed frequency of 2 years. The red line represents the GMST without climate intervention (SSM-SSP), whereas the blue line represents the GMST with climate intervention (SSM-ARISE). The orange line indicates the detrended GMST without climate intervention (SSM-SSP detrended), which is driven by the idealized ENSO in the SSM. See the Method section for a detailed description of the SSM.
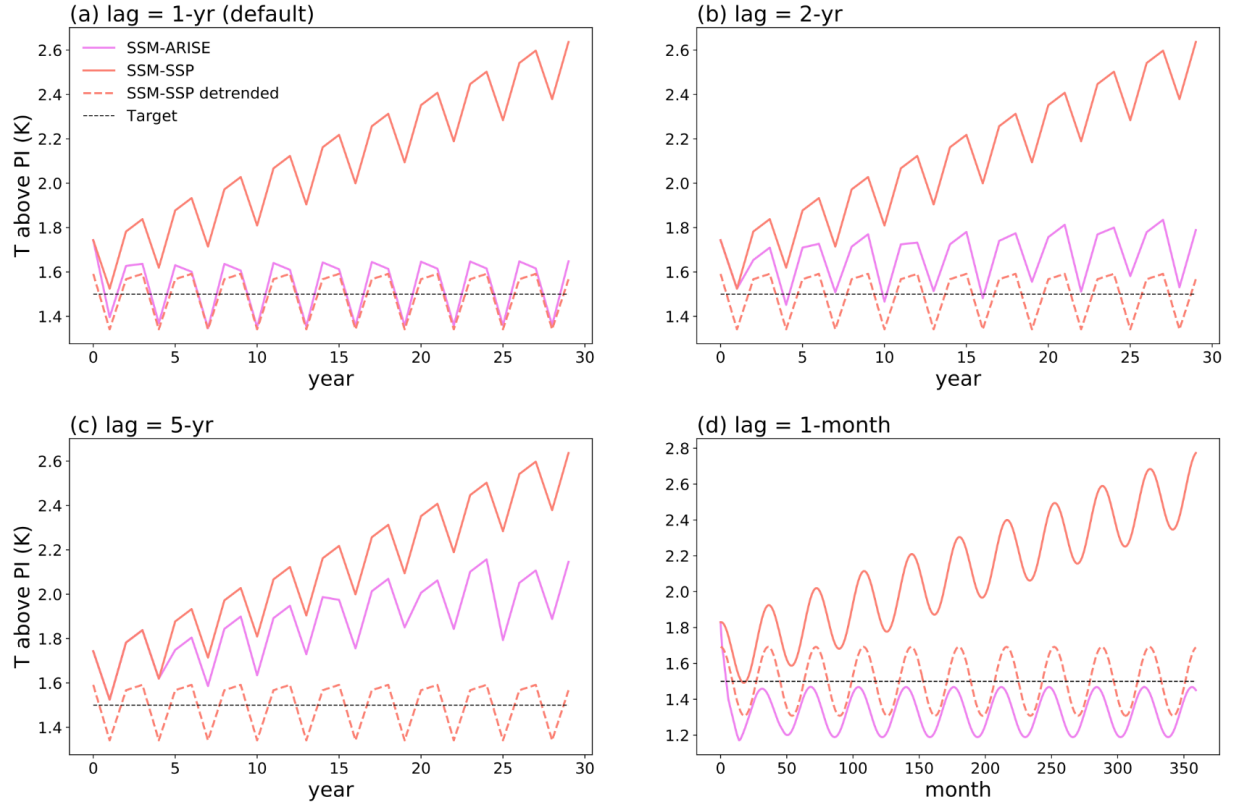
390

Figure 4. Similar to Fig 4b, but shows the climate intervention results based on the SSM with
different controller detection frequencies ranging from 1 month to 5 years. The frequency of the
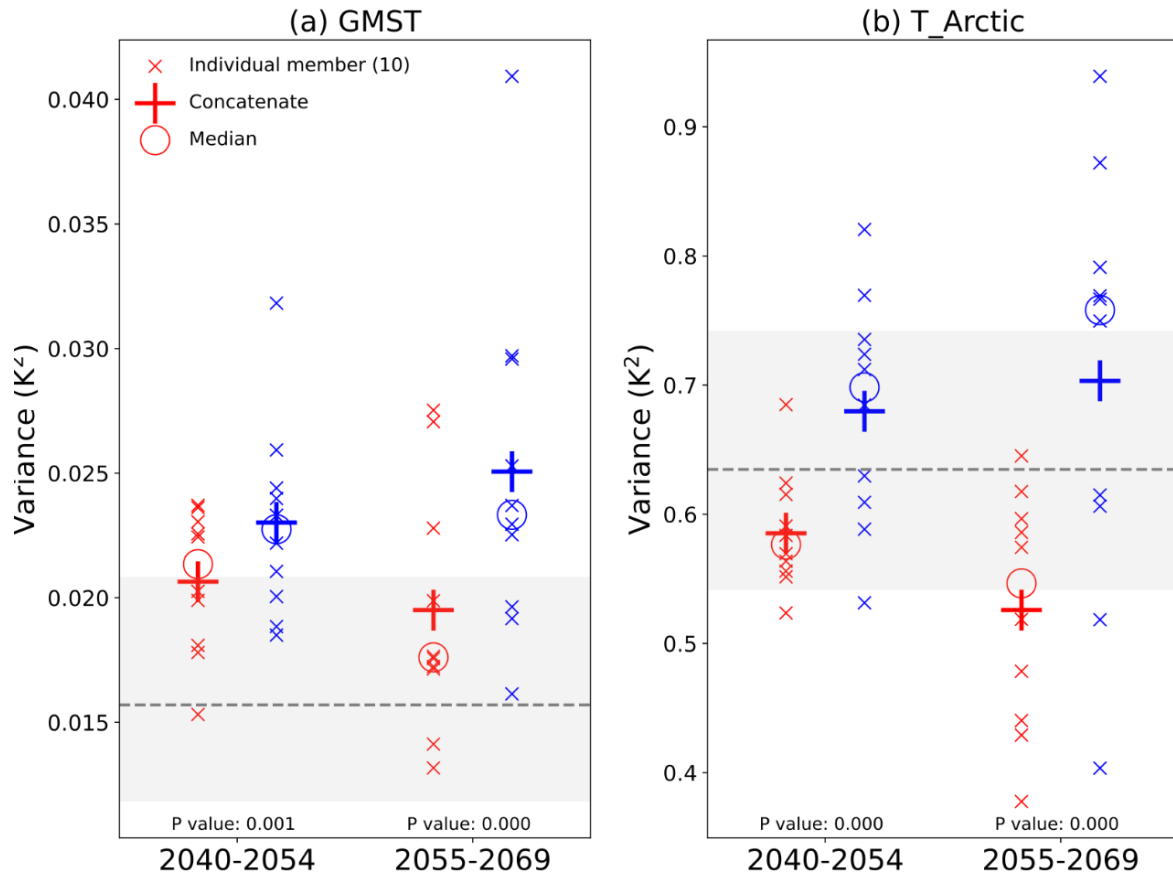idealized ENSO is fixed at three years in all four cases.

394

Figure 5. The variance of (a) annual global mean surface temperature (GMST) and (b) the annual Arctic surface temperature (T_Arctic) in SSP2-4.5 (red) and ARISE-SAI (blue) simulations for the period of (left) 2040–2054 and (right) 2055–2069. Cross marks represent the results of each individual ensemble member (10 in each simulation), whereas the circle marks represent the median. The plus marks indicate the variance of concatenated long-term GMST and T_Arctic. The grey shading and dashed line represent the variance spread of GMST for the target period of 2020-2035 from SSP2-4.5 and the variance of concatenated GMST, correspondingly.